A Comparison of Transition States During H-Atom Abstraction of Monophenols and Catechol by Methyl Radical

You-Min Sun[a] and Cheng-Bu Liu*[b]

Keywords: Activation energy / Catechol / Density functional calculations / H-atom abstraction / Monophenols

To compare the transition states of *para*-substituted phenols with that of catechol, we employed the B3LYP/6–311+G(d,p) method to calculate the energy profiles, the geometries, the spin density distributions, and other physico-chemical parameters. A comparison between catechol and *para*-substituted phenols indicates that their transition state geometries for hydrogen atom abstraction are similar. Substituent effects on the transition states of *o*-substituted phenols may differ from those of *p*-substituted ones. The calculated value of E_a for catechol is much lower than that of phenol, which arises mainly from the electron-donating property of the *ortho*-hydroxyl group. Although, the intramolecular hydrogen bond (IHB) effect on E_a is small, the IHB effect on the transition state geometry is fairly strong. According to the regression equation of the relative O–H bond dissociation enthalpy (BDE) versus values of E_a for *p*-substituted monophenols, the relative O–H BDE of catechol is –8.28 kcal mol^{-1}, which is in agreement with the value obtained through a kinetic analysis (–7.2 kcal mol^{-1}). The values of E_a are governed by resonance effects, which is similar to the observation found for the O–H BDEs.

Introduction

Phenolic antioxidants (ArOH) have been broadly applied in the food, pharmaceutical, and chemical industries to prevent oxidation induced by various radicals.[1−3] To select or design more-active ArOH compounds, we must understand the mechanisms of radical scavenging by ArOH. A great number of experimental and theoretical studies have been devoted to this topic.[4−14] It has been revealed that, in many cases, ArOH compounds scavenge free radicals, e.g., alkyl radicals (R•), by donating an H-atom directly.[13−16]

$$R^{\cdot} + ArOH \rightarrow RH + ArO^{\cdot}$$

It has been found that the O−H bond dissociation enthalpy (BDE), a thermodynamic parameter, is appropriate for characterizing the H-atom-abstracting ability, which provides a convenient criterion not only to evaluate the antioxidant activity but also to direct the design of better antioxidants.[17−27] To gain a complete knowledge of the radical scavenging process, however, we still have to understand the transition state (TS) pertaining to the H-atom abstraction reaction. Up to date, only a few of sporadic studies have been devoted to the TS for monophenols.[28−30] Although the relevant reaction profiles have been obtained, there are few comprehensive studies on the TS of phenols, especially on that of catechol.

Catechol is believed to be the active moiety in most natural antioxidants,[31−38] such as flavonoids, cinnamic acids, and coumarins. The value of the O−H BDE for catechol, however, has given rise to much controversy. By means of density functional theory (DFT) calculations on various basis sets, the O−H BDE for catechol was estimated to be 9.2 to 14.1 kcal mol^{-1} lower than that of phenol.[39−42] By employing the EPR equilibration technique, however, the value was estimated to be only −4.6 kcal mol^{-1} relative to that of phenol.[43] An intermediate value based on kinetic analysis was −6.9 kcal mol^{-1}.[44] Apparently, the disagreement cannot be reconciled until the TS for phenols, including catechol, is well understood, which stimulated us to undertake such a study.

In this article, we attempt, at first, to present a comprehensive theoretical study on the TS for phenols during H-atom abstraction by methyl radical, and then compare the TS of *para*-substituted phenols with that of catechol, which will be helpful to gain insight into the mechanism of radical scavenging by ArOH and to settle the dispute over the value of the O−H BDE of catechol.

Calculation Methods

Since the H-atom abstraction reaction is preferred in non-polar solvents, all calculations were conducted for the gas phase. For catechol and phenol, the geometries, includ-

[a] Institute of Theoretical Chemistry, Shandong University, Jinan, 250100, P. R. China
[b] Institute of Theoretical Chemistry, Shandong University, Jinan, 250100, P. R. China
Fax: (internat.) + 86-531-8564464
E-mail: tcsd@sdu.edu.cn

  DOI: 10.1002/ejoc.200300450

ing transition states, were calculated at first by DFT using the B3LYP function on the 6−31G(d,p) basis set,[45−47] and then on the B3LYP/6−311+G(d,p) level. For the *para*-substituted monophenols, full geometry optimization for the reactants, products, and transition states was performed on the B3LYP/6−311+G(d,p) level. For all energies, zero-point energy corrections have been included.

All stationary points were positively identified as minima or first-order saddle points by evaluation of the frequencies and normal modes. Furthermore, pathways between the transition states and their corresponding minima were characterized by calculations of intrinsic reaction coordinates (IRC).[48] Since the accuracy of DFT calculations depend also on the number of points used in the numerical integration in addition to the sources of numerical errors in the Hartree−Fock calculations, fine grids should be employed. In the present calculations, we used the default grid, which is a pruned (75, 302) grid that has 75 radical shell and 302 angular points per shell and results in about 7000 points per atom. All calculations were performed with the Gaussian 98 program package[49] on an SGI 300 server.

Results and Discussion

Basis Set Dependence of the Calculation Results

Since the HF methods give large spin contaminations in the treatment of aromatic radical systems and DFT approaches reasonably estimate the spin contamination, we chose the B3LYP DFT functional with two basis sets. The DFT-calculated structures of transition states with two basis sets for hydrogen atom (earmark $H^{\#}$) abstraction from phenol and catechol by methyl radical are similar to one another and the partial structural parameters of the transition states are listed in Table 1. Table 1 also lists the activation energies (E_a) for hydrogen atom abstraction from phenol and catechol. The value of E_a for catechol with the B3LYP/6−31G (d,p) method is calculated to be −0.77 kcal mol^{-1}, which suggests that DFT methods having a relative-low basis set will underestimate the energy and give much larger errors. The calculated results can be improved significantly by using the relatively larger basis set, 6−311+G(d,p). For example, the B3LYP/6−311+G(d,p)-calculated value of E_a for *p*-F-phenol is 4.56 kcal mol^{-1} (Table 6), which is in full agreement with the experimental value, 4.18 kcal mol^{-1}.[4] In fact, the standard 6−311+G(d,p) basis set is large enough to reduce the basis set superposition error inherent in the method, so that superposition error corrections become unnecessary. Based on the above discussion, we chose the B3LYP/6−311+G(d,p) method to conduct the calculations reported in this paper.

Table 1. Structural parameters and activation energies (E_a) for the transition states of phenol and catechol using the B3LYP method with two basis sets

Parameters	6−31G(d,p)		6−311+G(d,p)	
	Phenol	Catechol	Phenol	Catechol
$R_{O-H}^{\#}$ [Å]	1.124	1.085	1.129	1.109
$R_{C-H}^{\#}$ [Å]	1.427	1.510	1.421	1.468
$\theta_{C-H}^{\#}{}_{-O}$ [°]	172.65	174.37	179.30	175.80
O−H$^{\#}$−C−C torsion angle [°]	122.80	73.94	91.5	72.3
E_a [kcal mol^{-1}]	2.73	−0.77	5.43	2.70

Structures of Transition States

Schemes 1 and 2 present the geometries of the reactant, transition, and product states for phenol and catechol. The calculated results reveal that in the transition states, the O−H$^{\#}$ bond is elongated and the OH$^{\#}$−methyl radical distance is significantly shortened relative to the situation in the reactant states. The transferring hydrogen atom in the transition states is rotated out of the phenol ring plane by 91.5° for phenol and 72.3° for catechol (Table 1), which is in contrast with the reactant states where it is in the aromatic ring plane. The transferring hydrogen atom, the oxygen atom of the phenolic hydroxyl group, and the carbon atom of the methyl radical are nearly collinear, with the C−H$^{\#}$−O angles being 179.3 and 175.8° for the transition states of phenol and catechol, respectively.

Comparing the geometries in two transition states, we find that the O−H$^{\#}$ bond length in the transition state of phenol is longer and the C−H distance is shorter than those in catechol's transition state, but the sum of the O−H$^{\#}$ and C−H$^{\#}$ distances in both transition states is as high as ≈2.55 Å. For catechol, an intramolecular hydrogen bond (IHB) exists. We calculated the IHB distance in the transition state to be 2.134 Å, which is similar to the value in the reactant state (2.130 Å), but the value in the product state is much shorter (2.030 Å), which indicates that the strength of the IHB in the product state is stronger than that in the reactant state. This finding is consistent with the thermodynamic results obtained by the B3LYP/6−31G(d,p) method.[41,42]

Reaction Pathway Energy Profiles

The intrinsic reaction coordinate (IRC) was calculated to obtain the reaction pathway energy profiles for the H-atom abstraction, which are presented in Figure 1. A common feature in the profiles is that a hydrogen-bonded intermediate is formed from the isolated molecules and methyl radical before the formation of the transition state. In the progress of product formation, the hydrogen bonded phenoxyl−methane complex is formed initially, and then the isolated products are produced. The optimized structures of the intermediate hydrogen-bonded complexes and transition states are indicated in Schemes 1 and 2.

From the reaction pathway energy profiles in Figure 1 and Table 1, we see that the value of E_a for phenol is double that for catechol, which indicates that the H-atom abstraction from catechol is much easier than it is from phenol. This phenomenon arises apparently from catechol's *ortho*-hydroxyl group, which has two kinds of substituent effects

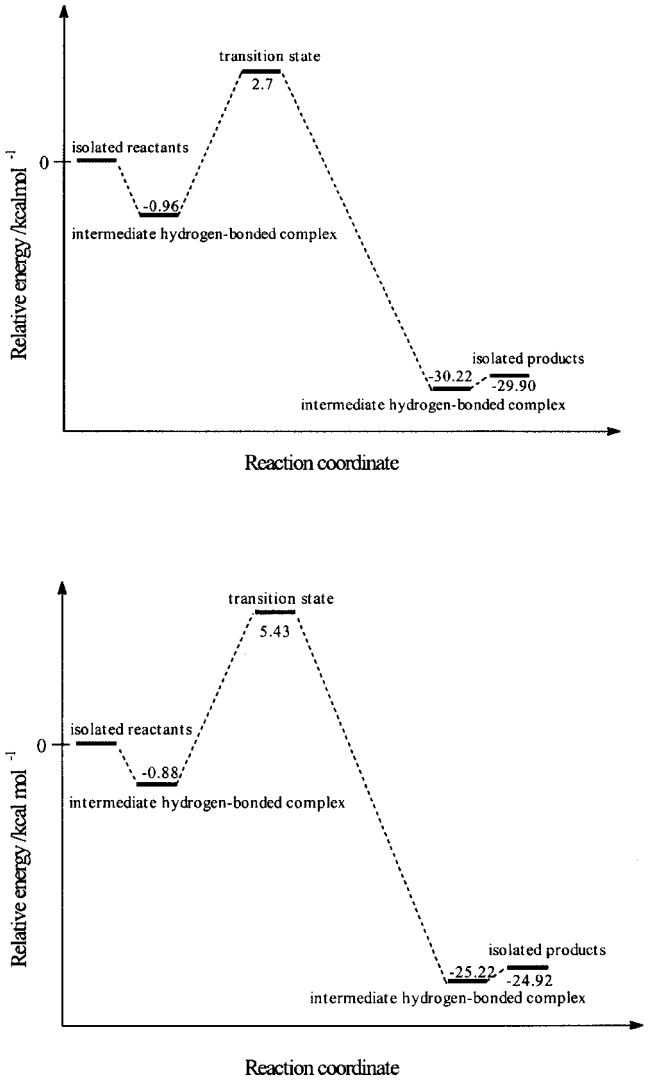

Figure 1. Reaction energy profile for hydrogen atom abstraction from catechol (top) and phenol (bottom) by the methyl radical

that reduce the value of E_a: the IHB effect and the *ortho*-hydroxyl electronic effect. To investigate these two effects, we located the transition state of non-hydrogen-bonded catechol at the B3LYP/6−311+G(d,p) level. The value of E_a for non-hydrogen-bonded catechol is calculated to be 3.05 kcal mol^{-1} (see Table 6), i.e., 2.38 kcal mol^{-1} lower than that of phenol, which reflects the electron-donating effect of the *o*-hydroxyl group. The difference between the values of E_a for the hydrogen-bonded and non-hydrogen-bonded forms of catechol is only 0.35 kcal mol^{-1}, which suggests that the IHB effect is small. As we see in Figure 1, the reaction enthalpy (ΔH) is negative, which suggests that the hydrogen atom abstraction is exothermic.

Spin Density and Electron Density Distributions in Transition States

Table 2 lists the unpaired spin density for the reactant, transition, and product states. From the reactants to the products, the electron transmission is through the carbon

Table 2. The unpaired spin density of the reactant state (RS), transition state (TS), and the product state (PS)

Spin density	Phenol			Catechol[a]		
	RS	TS	PS	RS	TS	PS
C atom[b]	1.0918	0.6744	0.0001	1.0850	0.6967	0.0006
H# atom	0.0213	−0.0040	0.0001	0.0322	0.0123	−0.0010
O atom[c]	0.0021	0.2522	0.4173	−0.0065	0.1967	0.3424

[a] Hydrogen-bonded form. [b] The C atom of the methyl radical. [c] The O atom from which the H atom is abstracted.

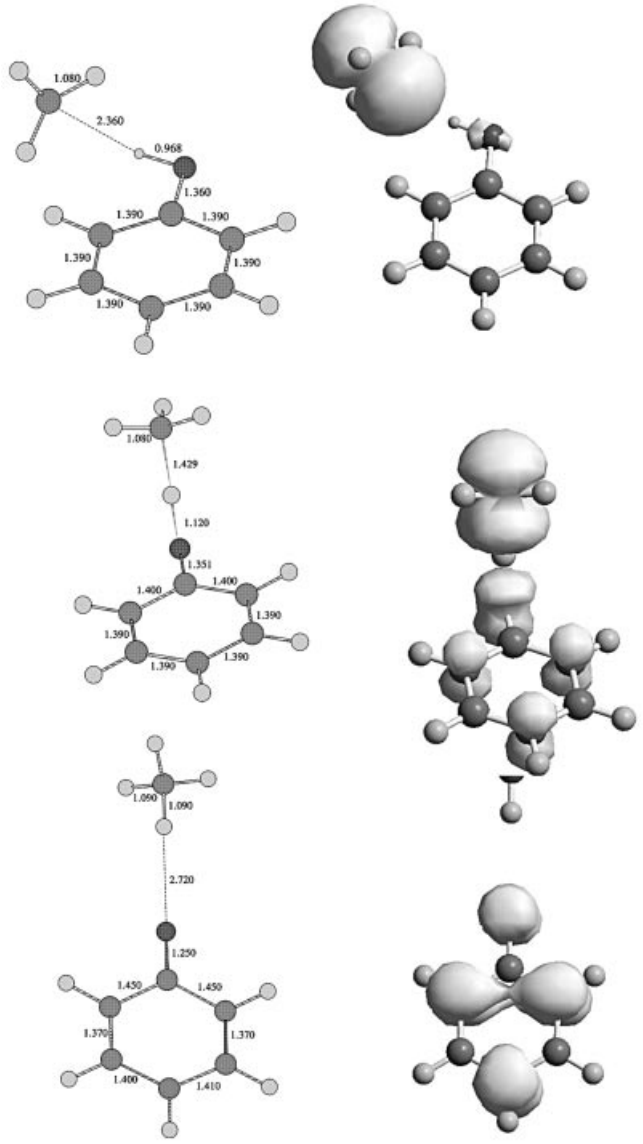

Scheme 1. The bond lengths (left; Å) and the unpaired spin density; distribution (right) for the reactant state (top), transition state (middle), and product state (bottom) for hydrogen atom transfer from phenol to the methyl radical

atom of the methyl radical to the oxygen atom of the phenoxyl radical. The transfer results indicate that the spin density of the carbon atom decreases, while the spin density of the oxygen atom increases. Scheme 1 demonstrates the mapping of the unpaired spin density distribution from the

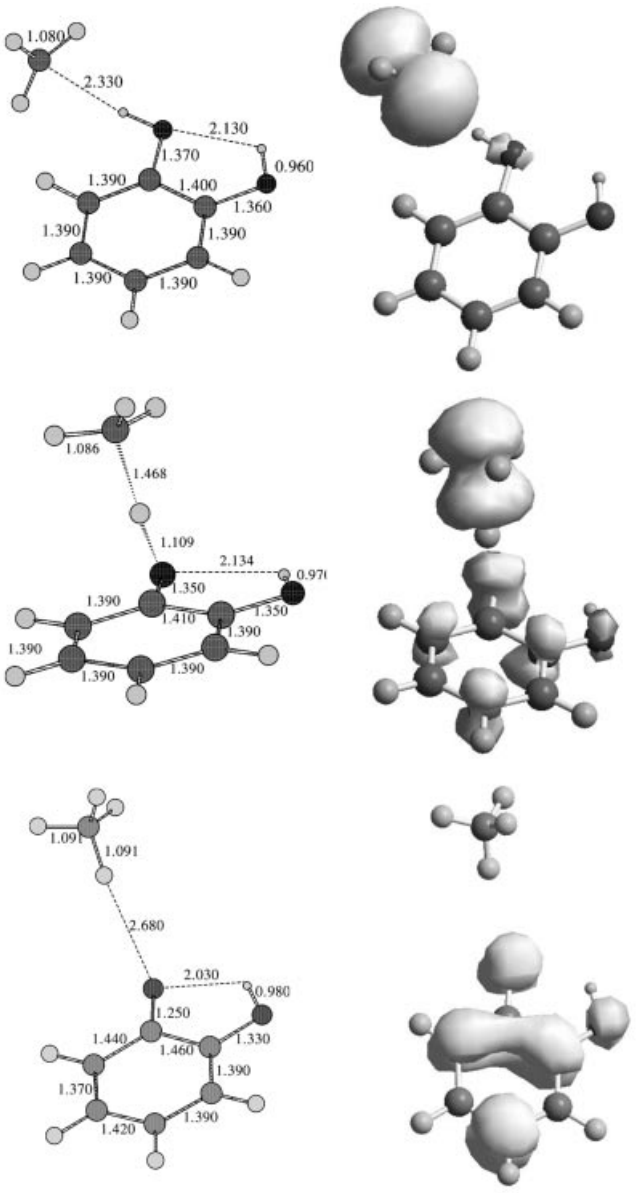

Scheme 2. The bond lengths (left; Å) and the unpaired spin density distribution (right) for the reactant state (top), transition state (middle), and product state (bottom) for hydrogen atom transfer from catechol to the methyl radical

reactants to the products for hydrogen atom transfer reaction from phenol to methyl radical. We find that the spin density resides on the carbon atom of the methyl radical in the reactants and resides on the phenoxyl radical and its conjugated phenyl ring in the products. In the transition states, however, the unpaired spin density is shared between the phenoxyl and methyl radicals. Similar results for catechol are displayed in Scheme 2.

Table 3 lists the calculated values of the electron densities on the hydrogen, oxygen, and carbon atoms, and on the O−H$^{\#}$ and C−O bonds as well. We observe variations of the electron densities during the reactions between the methyl radical and phenol or catechol. The electron densities of the carbon atoms in the reactions decrease, and those on the oxygen and *ipso*-carbon atom increase, upon progress toward the transition state. The change of the electron density of the hydrogen atom during the two reactions is somewhat different: they display, respectively, a decrease and an increase on moving toward the transition state. The electron densities of the carbon atom bound to the oxygen atom in the transition and product states for catechol are much higher than those in phenol. This observation is due to the electron density of the *ortho*-oxygen atom, which is delocalized throughout the phenyl ring and thereby stabilizes the transition state. This result is similar to the effect of electron-donating *para* substituents.[50]

Table 3. The electron densities on atoms and bonds

Electron density	Phenol			Catechol[a]		
	RS	TS	PS	RS	TS	PS
C atom[b]	5.2990	5.2518	4.9304	5.2967	5.2946	4.9331
C−H$^{\#}$ Bond	0.0206	0.2023	0.4018	0.0336	0.1553	0.3988
H$^{\#}$ atom	0.4667	0.3740	0.4018	0.4445	0.5149	0.49461
O−H$^{\#}$ Bond	0.2250	0.1888	0.0072	0.2081	0.0338	0.0004
O atom[c]	8.0864	8.1646	8.2461	8.1973	8.4119	8.2523
C* atom[d]	6.3163	6.8575	5.7930	8.5478	10.5839	9.0983

[a] Hydrogen-bonded form. [b] The C atom of the methyl radical. [c] The O atom from which the H atom is abstracted. [d] The C* atom that is bonded to the OH$^{\#}$ group.

The electron density of the O−H$^{\#}$ bond decreases from the reactant state to the product state. In contrast, the electron density of the C−H$^{\#}$ bond increases. This phenomenon makes it clear that the O−H$^{\#}$ bond is broken during the reaction and a new C−H$^{\#}$ bond is formed. Comparing the electron densities in both transition states, we see that the electron density of the O−H$^{\#}$ bond in the catechol transition state decreases more dramatically than that in the phenol transition state, which suggests that the breaking of the O−H$^{\#}$ bond in the reaction between catechol and methyl radical is much easier than that for phenol. The electron density of the newly formed C−H$^{\#}$ bond in the catechol transition state is smaller than that in the phenol transition state, which may arise from the fact that the C−H$^{\#}$ bond length in the catechol transition state (1.468 Å) is longer than that in the phenol transition state (1.421 Å; Table 1).

Effects of Substituents on Transition States

Table 4 lists structural parameters and spin densities on atoms for the transition states of *p*-substituted phenols. We find that the electron-donating substituents in phenol decrease the O−H$^{\#}$ bond length (r_1) and increase the C−H$^{\#}$ bond length (r_2), whereas electron-attracting substituents increase the value of r_1 and decrease the value of r_2. The plot of r versus values of E_a (Figure 2) indicates that the values of E_a increase with the elongation of r_1 and the shortening of r_2. If we add the values of r_1 and r_2 of catechol (including the hydrogen-bonded and non-hydrogen-bonded forms, which are illustrated by the red star and blue inverted-triangle points, respectively) to the two plots, we found, interestingly, that they are not positioned on the lin-

Table 4. Structural parameters and spin densities on atoms in the transition states

Substituents	O−H# bond length [Å]	C−H# bond length [Å]	Spin densities on H# atom	Spin densities on O atom	Spin densities on C atom[a]
H	1.129	1.421	−0.0040	0.2522	0.6744
CH_3	1.120	1.430	−0.0069	0.2416	0.6863
OCH_3	1.105	1.467	−0.0110	0.2230	0.7058
OH	1.107	1.462	−0.0103	0.2260	0.7036
NH_2	1.092	1.490	−0.0125	0.2029	0.7221
F	1.125	1.420	−0.0061	0.2481	0.6825
Cl	1.132	1.410	−0.0067	0.2543	0.6695
CHO	1.167	1.371	−0.0057	0.2992	0.6232
CN	1.162	1.370	−0.0054	0.2910	0.6314
NO_2	1.179	1.355	−0.0046	0.3159	0.6104
CF_3	1.159	1.370	−0.0076	0.2931	0.6365

[a] The C atom of the methyl radical.

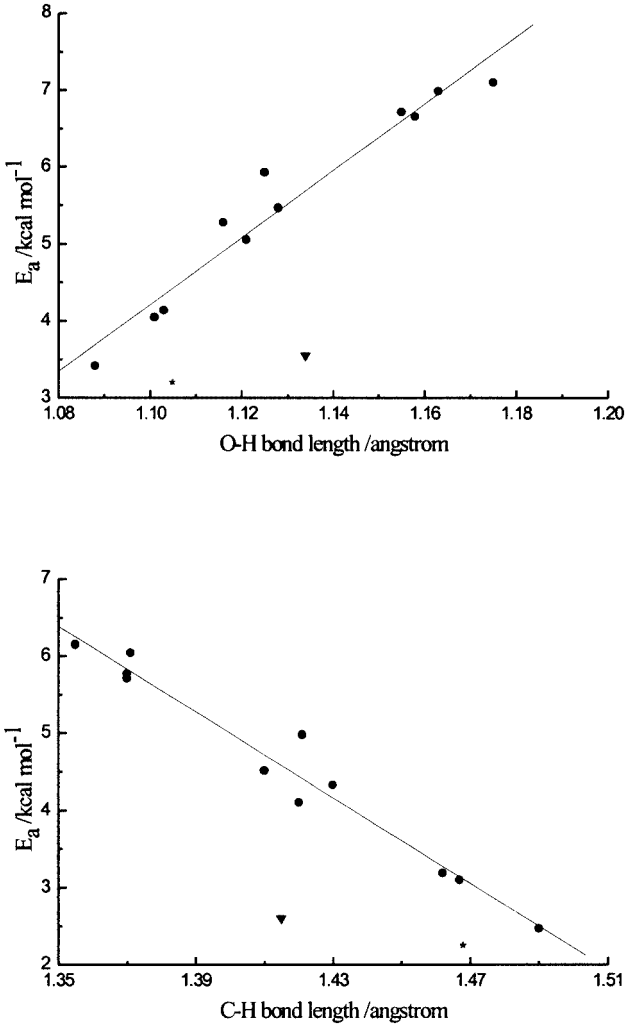

Figure 2. Correlation between the values of E_a and the O−H bond length (top, $r = 0.9733$) and C−H bond length (bottom, $r = -0.9817$) for phenols; the red star and blue inverted-triangle points indicate the values for the hydrogen-bonded and non-hydrogen-bonded catechols, respectively

ear regression lines. Analyzing the transition geometries for the OH-substituted phenols in the *ortho* and *para* positions, we find that some differences exist. The values of r_1 and r_2 for catechol (hydrogen-bonded form) are nearly the same as the corresponding values for *p*-OH-phenol, but the value of E_a of the former is lower than that of the latter as a result of the IHB effect. For the non-hydrogen-bonded form of catechol, the value of r_1 is much larger and that of r_2 is much smaller than the corresponding values for *p*-OH-phenol, but the difference between their values of E_a is only ca. 0.5 kcal mol^{-1}. Comparing the transition state geometries between the two forms of catechol, we find that the IHB effect on transition state geometry is rather strong. This observation suggests that the effect of substituents on transition states for the *o*-substituted phenols may differ from those of the *p*-substituted phenols, which is a situation that needs further verification by investigating the effects of substituents on the transition states of *o*-substituted phenols.

It is known that the unpaired spin density is shared between the phenoxyl groups and the methyl radical in the transition states. For phenols substituted by electron-donating groups, the spin density of the oxygen atom is lower and the spin density of the carbon atom is higher than those of phenol. Electron-attracting substituents, however, have an opposite effect. From these data, the linear relationships between the spin densities of the oxygen and carbon atoms are presented in Figure 3. If we add the values for catechol to the two plots, we observe, interestingly, that the hydrogen-bonded catechol (red star point) is on the regression line for the oxygen atom spin density, but not on the line for that of the carbon atom. The data point for the non-hydrogen-bonded catechol (blue inverted-triangle) is not on either of the two lines.

Table 5 lists the electron densities of atoms and bonds for the transition states. We attempted to plot the electron densities of atoms and bonds against the values of E_a. Linear relationships between the electron densities of the carbon atoms and the values of E_a, and the C−H# bonds and E_a, are presented in Figures 4 and 5. The corresponding values for catechol were also added to these plots, and we find that the values for the hydrogen-bonded catechol (red star) are on the line, but the values for the non-hydrogen-bonded catechol (blue inverted-triangle) are not. This observation further supports the notion that the effects of sub-

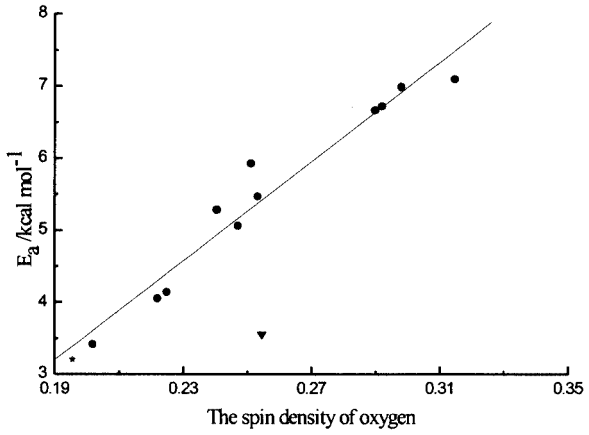

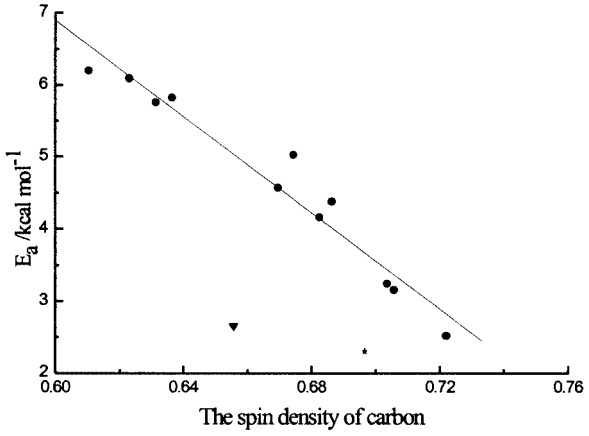

Figure 3. Correlation between the values of E_a and the spin density of the oxygen atom (top, $r = 0.9734$) and the spin density of the carbon atom (bottom $r = -0.9739$) for phenols; the red star and blue inverted-triangle points indicate the values for the hydrogen-bonded and non-hydrogen-bonded catechols, respectively

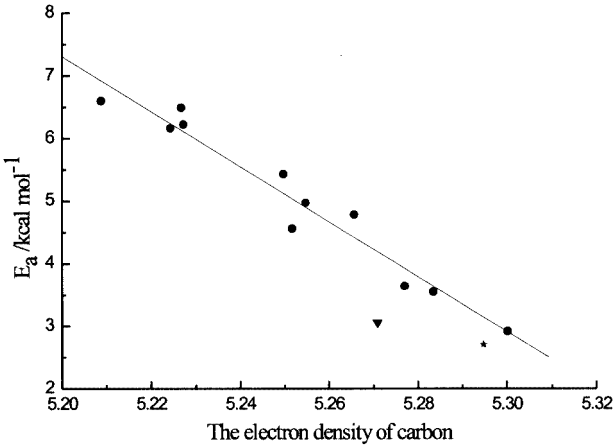

Figure 4. Correlation between the values of E_a and the electron density of the carbon atom ($r = -0.9754$); the red star and blue inverted-triangle points indicate the values for the hydrogen-bonded and non-hydrogen-bonded catechols, respectively

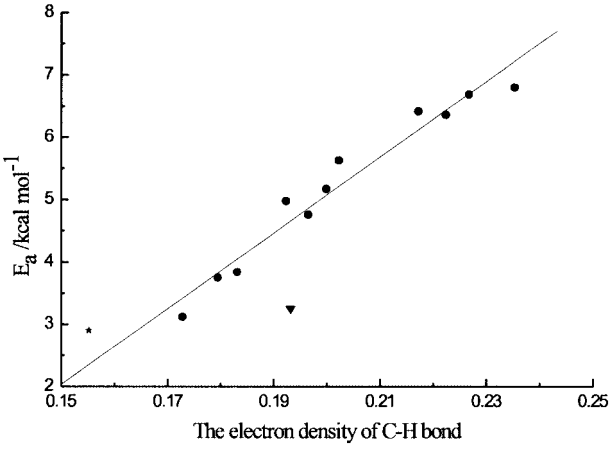

Figure 5. Correlation between the values of E_a and the electron density of the C−H bond ($r = 0.9768$); the red star and blue inverted-triangle points indicate the values of the hydrogen-bonded and non-hydrogen-bonded catechols, respectively

stituents on transition states for the *o*-substituted phenols may differ from those of the *p*-substituted phenols.

Table 6 lists the activation energies (E_a), relative O−H bond dissociation enthalpies (BDEs), logarithm of experimental rate constant (log k_H), and Hammett-type parameters σ_p^+ for *p*-substituted phenols and the corresponding values for catechol. We see that the presence of an electron-donating group in the *o*- or *p*-position in phenol reduces the values of E_a and increases the antioxidant activity, whereas the electron-attracting group increases the values

Table 5. The electron densities on atoms and bonds in the transition states

Substituents	C atom[a]	C−H# Bond	H# atom	O−H# Bond	O atom[b]	C−O bond	C* atom[c]
H	5.2518	0.2023	0.3740	0.1888	8.1646	0.5252	6.8575
CH_3	5.2677	0.1923	0.3707	0.1955	8.1601	0.5253	7.7564
OCH_3	5.2855	0.1795	0.3792	0.1949	8.1696	0.5387	7.3995
OH	5.2791	0.1831	0.3816	0.1925	8.1701	0.5449	7.2401
NH_2	5.3022	0.1729	0.3730	0.2080	8.1627	0.5691	7.2600
F	5.2538	0.1965	0.3861	0.1807	8.1718	0.5330	7.1099
Cl	5.2567	0.1999	0.4156	0.1597	8.1735	0.5507	8.5817
CHO	5.2288	0.2268	0.4594	0.1134	8.1744	0.5192	7.6131
CN	5.2263	0.2225	0.4610	0.1154	8.1750	0.5654	7.5043
NO_2	5.2107	0.2353	0.4718	0.1011	8.1770	0.5147	8.0318
CF_3	5.2293	0.2172	0.4582	0.12071	8.1756	0.5261	8.4509

[a] The C atom of the methyl radical. [b] The O atom from which the H atom is abstracted. [c] The C* atom that is bonded to the OH# group.

Table 6. The activation energy (E_a), the relative O−H BDE, the logarithm of the experimental rate constant (k_H), and Hammett-type parameters σ_p^+ for *p*-substituted phenols

Substituents	E_a [kcal mol^{-1}]	Relative O−H[a] BDE [kcal mol^{-1}]	log k_H[b]	σ_p^+[c]	F[c]	R^+[c]
H	5.43	0	3.63	0	0	0
CH_3	4.78	−1.81	4.13	−0.31	0.01	−0.32
OCH_3	3.55	−5.12	4.84	−0.78	0.29	−1.07
OH	3.64	−5.06	4.83	−0.92	0.33	−1.25
NH_2	2.92	−8.23		−1.30	0.08	−1.38
F	4.56	−1.89		−0.07	0.45	−0.52
Cl	4.97	−0.62	3.50	0.11	0.42	−0.31
CHO	6.49	2.37		0.73	0.33	0.40
CN	6.16	2.22	2.63	0.66	0.51	0.15
NO_2	6.60	4.21		0.79	0.65	0.14
CF_3	6.22	3.01		0.61	0.38	0.23
Catechol[d]	2.70 (2.64)[e]	−10.01	5.74			
Catechol[f]	3.05	−4.52				

[a] Data from ref.[42b] [b] The experienced values from ref.[51] [c] Data from ref.[52] [d] Hydrogen-bonded form. [e] Value in parenthesis was extrapolated from the regression equation. [f] Non-hydrogen-bonded form.

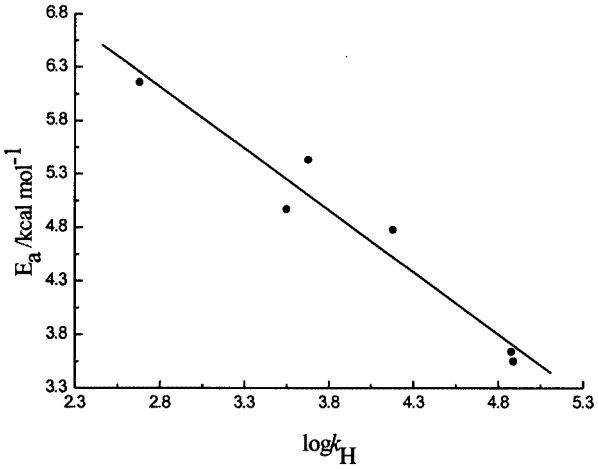

Figure 6. Correlation between log k_H and the calculated values of E_a for monophenols. The regression equation is: E_a = 9.30−1.16log k_H; r = −0.9714

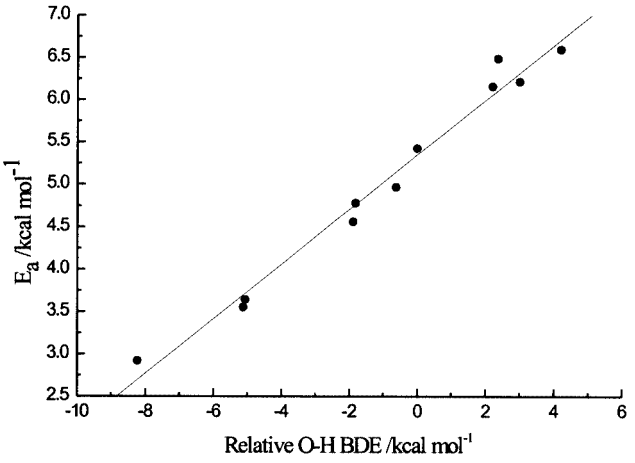

Figure 7. Correlation between the calculated values of E_a and the relative O−H BDE for monophenols. The regression equation is: E_a = 5.35 + 0.32 X, where X is the relative O−H BDE; r = 0.9901

of E_a and decreases the activity. Figure 6 is a plot of the calculated values of E_a versus the value of log k_H[51] for *p*-substituted monophenols. We find that a good linear relationship exists between log k_H and E_a. The regression equation is E_a = 9.30−1.16log k_H and the correlation coefficient (r) is 0.9742. According to the regression equation, the value of E_a of catechol was extrapolated to be 2.64 kcal mol^{-1}, which is consistent with the calculated result (2.70 kcal mol^{-1}).

The plot of the relative O−H BDE versus E_a shows that there also exits a linear relationship between them (r = 0.9901, Figure 7). Hence, it is rational to use the thermodynamic parameter O−H BDE to replace the value of E_a to predict the antioxidant activity of phenolic compounds. The resulting linear regression equation E_a = 5.35 + 0.32 X (where X is the relative O−H BDE) for *p*-substituted monophenols yields a relative O−H BDE for catechol of −8.28 kcal mol^{-1}, which is in fair agreement with the value obtained through a kinetic analysis (−7.2 kcal mol^{-1}).[44]

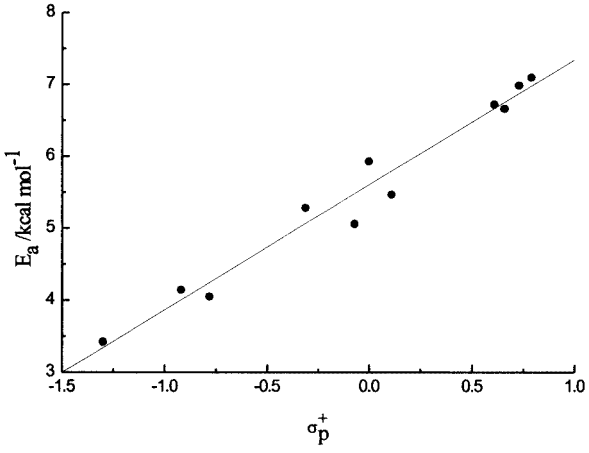

Figure 8. Correlation between the values of E_a and σ_p^+ for monophenols; r = 0.9833

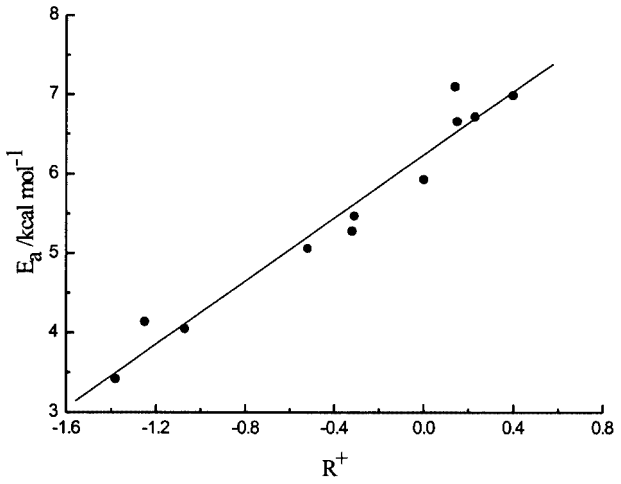

Figure 9. Correlation between the values of E_a and R^+ for monophenols; r = 0. 9764

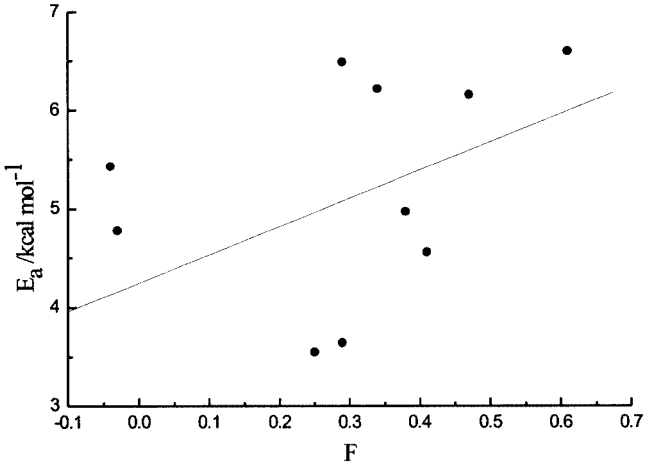

Figure 10. Correlation between the values of E_a and F for monophenols; r = 0.4663

Correlations between the Hammett-type parameter σ_p^+ [52] and the values of the O−H BDE of substituted phenols have been studied and good linear relationships have been observed.[53,54] Figure 8 indicates that a good correlation exists between σ_p^+ and the calculated values of E_a for the *p*-substituted monophenols (r = 0.9833). Because the value of σ_p^+ has two components, i.e., field/inductive (F) and resonance (R^+) parts ($\sigma_p^+ = F + R^+$),[52] it is interesting to determine whether the values of E_a are mainly governed by field/inductive effects or resonance effects. We find that the correlation between the values of E_a and R^+ (r = 0.9764) is much better than that between E_a and F (r = 0.4663) (Figures 9 and 10), which suggests that the values of E_a are governed by resonance effects. This result is similar to observations made on the values of the O−H BDEs.[24e,42b]

Conclusion

The B3LYP/6−311+G(d,p) method is a reliable method for locating transition states and calculating activation energies for phenols during H-atom abstraction. A comparison between the transition state geometries of catechol and *para*-substituted phenols indicates that similar transition states exist for these phenols during the process of donating one hydrogen atom. It is also interesting to observe that the effects of substituents on the transition states of *o*-substituted phenols may differ from those of *p*-substituted phenols. The calculated value of E_a of catechol is much lower than that of phenol, which mainly arises from the electron-donating property of the *ortho* hydroxyl group. Although the IHB effect on E_a is small, the IHB effect on the transition state geometry is rather strong. According to the regression equation of the relative O−H BDE versus the values of E_a of *p*-substituted monophenols, the relative O−H BDE of catechol was estimated to be −8.28 kcal mol^{-1}, which agrees with the value obtained by a kinetic analysis (−7.2 kcal mol^{-1}). In addition, we find that the values of E_a are governed by resonance effects, which is a similar finding to the observation regarding the O−H BDEs.

Acknowledgments

The authors are grateful to Prof. Hong-Yu Zhang (Shandong University of Technology) for his helpful assistance. This work was supported by the Natural Science Foundation of China (Grant nos. 20133020 and 20303011).

[1] G. W. Burton, K. U. Ingold, *Acc. Chem. Res.* **1986**, *19*, 194−201.
[2] V. W. Bowry, K. U. Ingold, *Acc. Chem. Res.* **1999**, *32*, 27−34.
[3] G. Scott, *Bull. Chem. Soc. Jpn.* **1988**, *61*, 165−170.
[4] P. Franchi, M. Lucarini, G. F. Pedulli, L. Valgimigli, B. Lunelli, *J. Am. Chem. Soc.* **1999**, *121*, 507−514.
[5] C. Evans, J. C. Scaiano, K. U. Ingold, *J. Am. Chem. Soc.* **1992**, *114*, 4589−4593.
[6] D. Ruegge, H. Fischer, *Int. J. Chem. Kinet.* **1989**, *21*, 703−714.
[7] E. Migliavacca, P. A. Carrupt, B. Testa, *Helv. Chim. Acta* **1997**, *80*, 1613−1626.
[8] S. Tomiyama, S. Sakai, T. Nishiyama, F. Yamada, *Bull. Chem. Soc. Jpn.* **1993**, *66*, 299−304.
[9] K. Mukai, K. Daifuku, K. Okabe, T. Tanigaki, K. Inoue, *J. Org. Chem.* **1991**, *56*, 4188−4195.
[10] T. G. Denisova, E. T. Denisov, *Polym. Degrad. Stabil.* **1998**, *60*, 345−350.
[11] B. Ahrens, M. G. Davidson, V. T. Forsyth, M. F. Mahon, A. L. Johnson, S. A. Mason, R. D. Price, P. R. Raithby, *J. Am. Chem. Soc.* **2001**, *123*, 9164−9165.
[12] S. Nagaoka, A. Kuranaka, H. Tsuboi, U. Hagashima, K. Mukai, *J. Phys. Chem.* **1992**, *96*, 2754−2761.
[13] V. Bondet, W. Brand-Williams, C. Berset, *Lebensm.-Wiss. Technol.* **1997**, *30*, 609−615.
[14] M. I. de Heer, P. Mulder, H.-G. Korth, K. U. Ingold, J. Lusztyk, *J. Am. Chem. Soc.* **2000**, *122*, 2355−2360.
[15] G. W. Burton, Y. Le Page, E. J. Gabe, K. U. Ingold, *J. Am. Chem. Soc.* **1980**, *102*, 7791−7792.
[16] G. W. Burton, T. Doba, E. J. Gabe, L. Hughes, F. L. Lee, L. Prasad, K. U. Ingold, *J. Am. Chem. Soc.* **1985**, *107*, 7053−7065.
[17] R. M. Borges dos Santos, J. A. Martinho Simoes, *J. Phys. Chem. Ref. Data* **1998**, *27*, 707−739.
[18] H. Y. Zhang, *J. Am. Oil Chem. Soc.* **1999**, *76*, 745−748.
[19] M. Lucarini, G. F. Pedulli, M. Cipollone, *J. Org. Chem.* **1994**, *59*, 5063−5070.
[20] L. J. J. Laarhoven, P. Mulder, D. D. Wayner, *M. Acc. Chem. Res.* **1999**, *32*, 342−349.
[21] Y. D. Wu, D. K. W. Lai, *J. Org. Chem.* **1996**, *61*, 7904−7910.

[22] J. S. Wright, D. J. Carpenter, D. J. McKay, K. U. Ingold, *J. Am. Chem. Soc.* **1997**, *119*, 4245−4252.
[23] G. A. DiLabio, D. A. Pratt, A. D. LoFaro, J. S. Wright, *J. Phys. Chem. A* **1999**, *103*, 1653−1661.
[24] [24a] Y. M. Sun, H. Y. Zhang, D. Z. Chen, C. B. Liu, *Org. Lett.* **2002**, *4*, 2909−2911. [24b] Y. M. Sun, H. Y. Zhang, D. Z. Chen, *Chin. J. Chem.* **2001**, *19*, 657−661. [24c] Y. M. Sun, X. L. Wang, H. Y. Zhang, D. Z. Chen, *Quant. Struct.-Act. Relat.* **2001**, *20*, 139−142. [24d] Y. M. Sun, D. Z. Chen, C. B. Liu, *J. Mol. Struct. (Theochem)* **2002**, *618*, 181−189. [24e] H. Y. Zhang, Y. M. Sun, D. Z. Chen, *Quant. Struct.-Act. Relat.* **2001**, *20*, 148−152.
[25] D. A. Pratt, G. A. DiLabio, G. Brigati, G. F. Pedulli, L. Valgimigli, *J. Am. Chem. Soc.* **2001**, *123*, 4625−4626.
[26] H. Y. Zhang, L. F. Wang, *Bioorg. Med. Chem. Lett.* **2002**, *12*, 225−227.
[27] H. Y. Zhang, L. F. Wang, *Bioorg. Med. Chem. Lett.* **2003**, *13*, 909−911.
[28] K. Tanaka, S. Sakai, S. Tomiyama, T. Nishiyama, F. Yamada, *Bull. Chem. Soc. Jpn.* **1991**, *64*, 2677−2680.
[29] J. O. Patrick, *Chem. Lett.* **2002**, *364*, 318−322.
[30] O. Tishchenko, E. S. Kryachko, M. T. Nguyen, *J. Mol. Struct.* **2002**, *615*, 247−250.
[31] S. A. B. E. van Acker, M. J. de Groot, D.-J. van dern Berg, M. N. L. Trop, G. D.-O. den Kelder, W. J. F. van der Vijhg, A. Bast, *Chem. Res. Toxicol.* **1996**, *9*, 1305−1312.
[32] V. A. Roginsky, T. K. Barsukova, A. A. Remorova, W. Bors, *J. Am. Oil Chem. Soc.* **1996**, *73*, 777−786.
[33] M. Foti, M. Piattelli, M. T. Baratta, G. Ruberto, *J. Agric. Food. Chem.* **1996**, *44*, 497−501.
[34] A. Arora, M. G. Nair, G. M. Strasburg, *Free Radic. Biol. Med.* **1998**, *24*, 1355−1363.
[35] S. V. Jovanovic, S. Steenken, M. Tosic, B. Marjanovic, M. G. Simic, *J. Am. Chem. Soc.* **1994**, *116*, 4846−4851.
[36] C. A. Rice-Evans, N. J. Miller, G. Paganga, *Free Radical Biol. Med.* **1996**, *20*, 933−956.
[37] M. Ogata, M. Hoshi, K. Shimotohno, S. Urano, T. Endo, *J. Am. Oil Chem. Soc.* **1997**, *74*, 557−562.
[38] P.-G. Pietta, *J. Nat. Prod.* **2000**, *63*, 1035−1042.
[39] F. Hino, L. A. Eriksson, M. R. A. Blomberg, P. E. M. Siegbahn, *Int. J. Quantum Chem.* **2000**, *76*, 714−723.
[40] J. S. Wright, E. R. Johnson, G. A. DiLabio, *J. Am. Chem. Soc.* **2001**, *123*, 1173−1183.
[41] The IHB strength for the catechol radical and the parent catechol were calculated to be 9.58 and 4.1 kcal mol^{-1}, respectively. See refs.[42a,42b]
[42] [42a] H.-G. Korth, M. I. de Heer, P. Mulder, *J. Phys. Chem. A* **2002**, *106*, 8779−8789. [42b] H. Y. Zhang, Y. M. Sun, X. L. Wang, *Chem. Eur. J.* **2003**, *9*, 502−508.
[43] M. Lucarini, V. Mugnaini, G. F. Pedulli, *J. Org. Chem.* **2002**, *67*, 928−931.
[44] H. Y. Zhang, *New J. Chem.* **2003**, *27*, 453−454.
[45] C. Lee, W. Yang, R. G. Parr, *Phys. Rev. B.* **1988**, *37*, 785−789.
[46] P. J. Stevenes, F. J. Devlin, C. F. Chabalowski, M. J. Frisch, *J. Phys. Chem.* **1994**, *98*, 11623−11627.
[47] A. D. Becke, *J. Chem. Phys.* **1993**, *98*, 1372−1377.
[48] K. Fukui, *J. Phys. Chem.* **1970**, *74*, 4161−4163.
[49] M. J. Frisch, G. W. Trucks, H. B. Schlegel, P. M. W. Gill, B. G. Johnson, M. A. Robb, J. R. Cheeseman, T. Keith, G. A. Petersson, J. A. Montgomery, K. Raghavachari, M. A. Al-Laham, V. G. Zakrzewski, J. V. Ortiz, J. B. Foresman, C. Y. Peng, P. Y. Ayala, W. Chen, M. W. Wong, J. L. Andres, E. S. Replogle, R. Gomperts, R. L. Martin, D. J. Fox, J. S. Binkley, D. J. Defrees, J. Baker, J. P. Stewart, M. Head-Gordon, C. Gonzalez, J. A. Pople, *Gaussian 98, Revision A.9,* Gaussian, Inc., Pittsburgh, PA, **1999**.
[50] S. A. B. E. van Acker, L. M. H. Koymans, A. Bast, *Free Radical Biol. Med.* **1993**, *15*, 311−328.
[51] M. C. Foti, E. R. Johnson, M. R. Vinqvist, J. S. Wright, L. R. C. Barclay, K. U. Ingold, *J. Org. Chem.* **2002**, *67*, 5190−5196.
[52] C. Hansch, A. Leo, R. W. Taft, *Chem. Rev.* **1991**, *91*, 165−195.
[53] A. K. Chandra, T. Uchimaru, *Int. J. Mol. Sci.* **2002**, *3*, 407−422.
[54] L. J. J. Laarhover, I. W. C. E. Arends, P. Mulder, *J. Anal. Appl. Pyrolysis* **2000**, *54*, 153−192.

Received July 21, 2003

